

Interfacial confinement in core-shell nanowires due to high dielectric mismatch

A. A. Sousa, T. A. S. Pereira, A. Chaves, J. S. de Sousa, and G. A. Farias

Citation: *Appl. Phys. Lett.* **100**, 211601 (2012); doi: 10.1063/1.4720402

View online: <http://dx.doi.org/10.1063/1.4720402>

View Table of Contents: <http://apl.aip.org/resource/1/APPLAB/v100/i21>

Published by the [American Institute of Physics](http://www.aip.org).

Related Articles

Surface effect on electronic and optical properties of Bi₂Ti₂O₇ nanowires for visible light photocatalysis
J. Appl. Phys. **111**, 124306 (2012)

Electronic properties of embedded MnAs nano-clusters in a GaAs matrix and (Ga,Mn)As films: Evidence of distinct metallic character
Appl. Phys. Lett. **100**, 203121 (2012)

Communication: Electronic band gaps of semiconducting zig-zag carbon nanotubes from many-body perturbation theory calculations
J. Chem. Phys. **136**, 181101 (2012)

Electronic and optical properties of free-standing and supported vanadium nanowires
J. Appl. Phys. **111**, 093506 (2012)

Electronic and structural properties of InAs/InP core/shell nanowires: A first principles study
J. Appl. Phys. **111**, 054315 (2012)

Additional information on *Appl. Phys. Lett.*

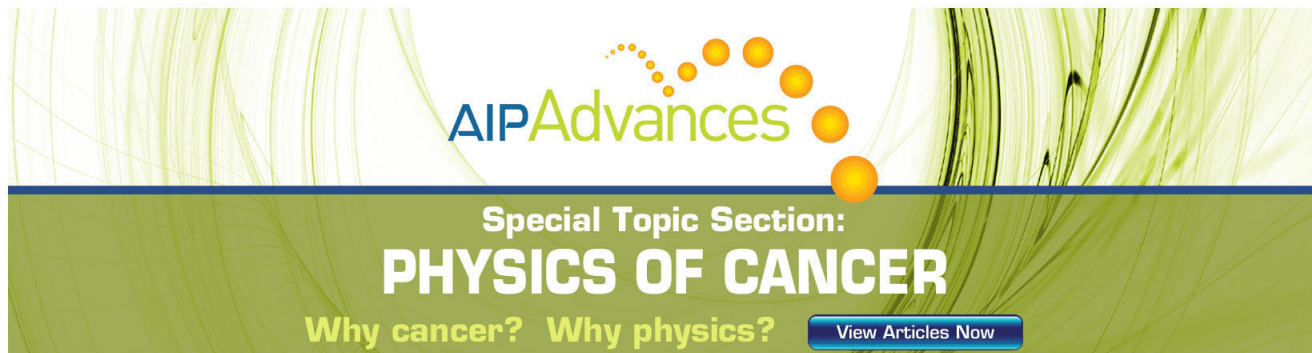
Journal Homepage: <http://apl.aip.org/>

Journal Information: http://apl.aip.org/about/about_the_journal

Top downloads: http://apl.aip.org/features/most_downloaded

Information for Authors: <http://apl.aip.org/authors>

ADVERTISEMENT



AIP Advances

Special Topic Section:
PHYSICS OF CANCER

Why cancer? Why physics? [View Articles Now](#)

Interfacial confinement in core-shell nanowires due to high dielectric mismatch

A. A. Sousa,¹ T. A. S. Pereira,¹ A. Chaves,² J. S. de Sousa,² and G. A. Farias²

¹*Institute of Physics, Federal University of Mato Grosso, 78060-900 Cuiabá, Mato Grosso, Brazil*

²*Department of Physics, Federal University of Ceará, C.P. 6030, 60455-900 Fortaleza, Ceará, Brazil*

(Received 14 March 2012; accepted 5 May 2012; published online 22 May 2012)

We theoretically investigate the role of the dielectric mismatch between materials on the energy levels and recombination energies of a core-shell nanowire. Our results demonstrate that when the dielectric constant of the core material is lower than that of the shell material, the self-image potential pushes the charge carriers towards the core-shell interface in such a way that the ideal confinement model is no longer suitable. The effects of this interfacial confinement on the electronic properties of such wires, as well as on its response to applied magnetic fields, are discussed. © 2012 American Institute of Physics. [<http://dx.doi.org/10.1063/1.4720402>]

Great attention has been devoted to the investigation of the electronics and optical properties of core-shell nanowires (NW). In particular, the applications of these low dimensional structures in optoelectronic and photonic devices are of interest for the electronics industry, and much effort has been dedicated to their fabrication.¹⁻⁴ In addition, studies of low dimensional systems surrounded by high dielectric constant materials continue to attract attention from many researchers^{5,6} towards a continuation of the Moore's law. Recently, wire diameters of a few nanometers were experimentally achieved,⁷ and carrier confinement effects in these nanowires have been reported with different levels of sophistication.⁸⁻¹⁰

This work aims to investigate the dielectric mismatch effects on core-shell NW, focusing on the possibility of interfacial confinement of the carriers. As for the model structure, we consider a semiconductor cylindrical nanowire (core region) of radius R , surrounded by a different material (shell region). The interface between core and shell regions is assumed to be abrupt, i.e., the materials parameters change abruptly from the core to the shell regions. For the heterostructure materials considered in this paper, the bands mismatch creates a high potential barrier for the charge carriers in the shell, leading to a short penetration of the wave functions in this region. This rules out the role of the shell width on the energy states of the NW since the wave function does not reach the outer edge of the shell. The nanowire electronic structure is obtained by solving numerically a Schrödinger-like equation within the adiabatic approach and the effective mass framework.¹¹ The total confinement potential $V_T^i(\rho_i) = \Delta E_i(\rho_i) + \Sigma_i(\rho_i)$ is given by the sum of band edges discontinuities $\Delta E_i(\rho_i)$ and the self-energy potential $\Sigma_i(\rho_i)$, where $i = e, lh, hh$ represents the carrier types (electron, light hole, and heavy hole, respectively). The latter term appears due to the dielectric mismatch, and its calculation is based on the method of the image charges. The details of this calculation can be seen in our supplementary material.¹¹ In a nutshell, the self-energy potential $\Sigma_i(\rho_i)$ inside the core region, due to a carrier located in the core region, is given by Eq. (19) of Ref. 10, whereas when the carrier is located in the shell region, the self-energy potential inside this region can be obtained using a similar expression, just

by changing the modified Bessel functions of the first type, $I_m^2(k\rho_e)$ and $I_m^2(k\rho_h)$, by those of the second type, $K_m^2(k\rho_e)$ and $K_m^2(k\rho_h)$, respectively.

The electron-hole recombination energy, $E_R^{e-h} = E_G + E_e + E_h$ ($h = lh$ or hh), given by the sum of the band gap energy E_G on the core region with the electron E_e and hole E_h confinement energies, is calculated for the radial ground state quantum number $n = 1$ and zero angular momentum $l = 0$, allowing us to analyze the effects caused by the self-energy potential on the ground state energy of the electron-hole pair. Figure 1(a) shows the role of the dielectric mismatch on the value of the electron-hole recombination energy $\Delta E_R^{e-h} = E_{R,\Sigma_i(\rho_i) \neq 0} - E_{R,\Sigma_i(\rho_i) = 0}$, as a function of the ratio $\varepsilon_r = \varepsilon_1/\varepsilon_2$ between dielectric constants of the core (ε_1) and shell (ε_2) materials, considering several values of nanowire radii R , for different materials. This quantity denotes the difference between the recombination energies with ($E_{R,\Sigma_i(\rho_i) \neq 0}$) and without ($E_{R,\Sigma_i(\rho_i) = 0}$) the self-energy corrections. The analysis of this difference gives us the advantage of excluding the effect of quantum confinement due to the band edge mismatch ΔE_i , remaining exclusively the confinement due to the dielectric mismatch. The material parameters are the same as in Ref. 12.

As in the case of quantum wells, shown by Pereira *et al.*,¹² if the dielectric constant in core region ε_1 is smaller than that of the shell region ε_2 , the potential in the core region is attractive and its contribution to the recombination energy is negative $\Delta E_R < 0$. On the other hand, for a larger dielectric constant in core region, as compared to the one in the shell region, the potential in the core region is repulsive, so that its contribution to the recombination energy is positive $\Delta E_R > 0$, as clearly shown in Fig. 1(a). The resulting ΔE_R^{e-h} for both light and heavy holes are the same, as this quantity only contains the effects of $\Sigma_i(\rho_i)$ on the carrier charge. On the other hand, by plotting E_R^{e-h} , it is possible to observe the difference between $e-lh$ and $e-hh$ pairs, caused by the different light hole and heavy hole effective masses.

Note that the AlGaAs/GaAs heterostructure has $\varepsilon_r \approx 1$, i.e., the dielectric mismatch in this case is negligible. In fact, one can verify in Fig. 1(a) that for AlGaAs/GaAs, $\Delta E_R \approx 0$ for any value of wire radius. AlGaAs/GaAs core-shell wires

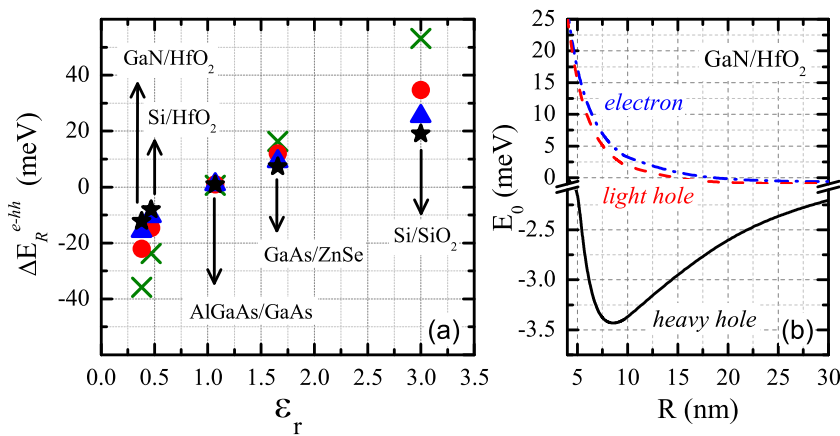


FIG. 1. (a) Effect of the self-energy potential on the recombination energy of an electron-hole pair, for different wire radii: 4 nm (\times), 6 nm (\bullet), 8 nm (\blacktriangle), and 10 nm (\blacksquare). (b) Ground state energies as a function of the core radius for carriers confined in a GaN/HfO₂ core-shell heterostructure.

have been widely experimentally studied for many reasons, e.g., the possibility of obtaining lattice matched defect-free samples, where the AlGaAs shell reduces the surface-related nonradiative recombination, by passivating the GaAs core.¹³ However, the results in Fig. 1(a) suggest that this heterostructure is actually not the best choice for investigating dielectric mismatch effects. As we will demonstrate onwards, the case of GaN/HfO₂ heterostructures is particularly interesting.

The growth of nitride-based cylindrical core wires,⁷ as well as HfO₂ shells,⁶ has been reported recently, which makes us believe that such a structure could be experimentally realized in near future. Figure 1(b) shows the ground state energies E_0 (i.e., for $n=1$ and $l=0$) for each carrier in a core-shell GaN/HfO₂ heterostructure as a function of the core radius. As usual, as the radius increases, the carrier confinement becomes weaker, leading to a reduction in the ground state energy, which is clearly observed for the electron and the light hole in this case. Conversely, the heavy hole energy shows a non-monotonic dependence on the radius, namely, it decreases for smaller radii but starts to increase as the radius becomes larger, suggesting a different confinement regime for this carrier. In fact, such a behavior is analogous to the one reported in the literature for GaN/HfO₂ quantum wells.¹⁴ In the quantum wells case, such a non-monotonic behavior of the confinement energy was demonstrated to be a consequence of the fact that $\epsilon_r < 1$ in this heterostructure, leading to an attractive potential which pulls the carrier towards the interface between the materials. Analogously, this suggests the existence of an interfacial confinement of the heavy hole in the NW. For smaller radii, the quantum confinement due to the bands mismatch is still dominant, but as the radius is enlarged, the energy decreases and eventually enters the negative energy domain, where the hh becomes bound to the core-shell interface due to the self-image potential. Being compressed towards the interface, the hh experiences an increase in its energy as the radius is further enlarged.

Notice that the sign of the confinement energy indicates whether a charge carrier is confined in the core or at the interfacial region. Without dielectric mismatch, or even for $\epsilon_r > 1$, the confinement energy is always positive since the bottom of the confinement potential V_T^i is always either zero or larger. Conversely, the presence of a $\epsilon_r < 1$ mismatch is responsible for negative cusps on the potential at

the interfacial region.^{10,12} Hence, a negative confinement energy suggests an interfacial confinement. In fact, the heavy hole is the only carrier with negative energy in Fig. 1(b), and it is indeed the only one exhibiting non-monotonic behavior of the confinement energy as the radius increases.

The consequences of the interfacial confinement are numerous. For instance, for some combinations of core-shell materials, one might find holes in the interface and electrons in the core. Such an electron-hole spatial separation leads to a reduction of the overlap between their wavefunctions, reducing the oscillator strength and, consequently, the recombination rate. The overlaps between electron and light (lh , top) and heavy (hh , bottom) hole wave functions are shown as a function of the core wire radius R in Fig. 2(a), for the same combinations of core and shell materials in Fig. 1(a). For all the heterostructures shown, the overlap value is slightly lower than unit for small radii. This is just a consequence of the fact that wave functions for different charge carriers penetrate with different depths into the barriers, and this effect is more pronounced when the NW radius is small. In the AlGaAs/GaAs (blue), GaAs/ZnSe (green), and Si/SiO₂ (black) cases, where the dielectric constants ratios are $\epsilon_r > 1$, the overlaps for both $el-lh$ and $el-hh$ pairs simply converge to 1 as the radius increases, which means that electrons and holes are practically equally distributed in space for larger wire radius. However, the overlaps in the $\epsilon_r < 1$ heterostructures exhibit a maximum at moderate R (around 10–20 nm) and decrease after this value, indicating different distributions of electron and holes functions for large R . Although this effect is also present for the Si/HfO₂ heterostructure, it is much stronger in the GaN/HfO₂ case (red), specially for the $el-hh$ pair.

In order to help us to understand the heavy hole interfacial confinement and the consequently different spatial distribution of charge carriers, Fig. 2(b) illustrates the total confinement potential (black solid), along with the normalized ground state wave functions, for electrons (top) and heavy holes (bottom) in a $R=30$ nm GaN/HfO₂ core-shell NW. The electron wave function considering dielectric mismatch effects (black dashed) is still confined mostly in the vicinity of the central axis of the core, even at such a large radius, and its width is wider than that without dielectric mismatch (blue dash dotted). On the other hand, the heavy hole wave functions, depicted in the bottom panel of Fig. 2(b) for different values of the core wire radius R , are clearly

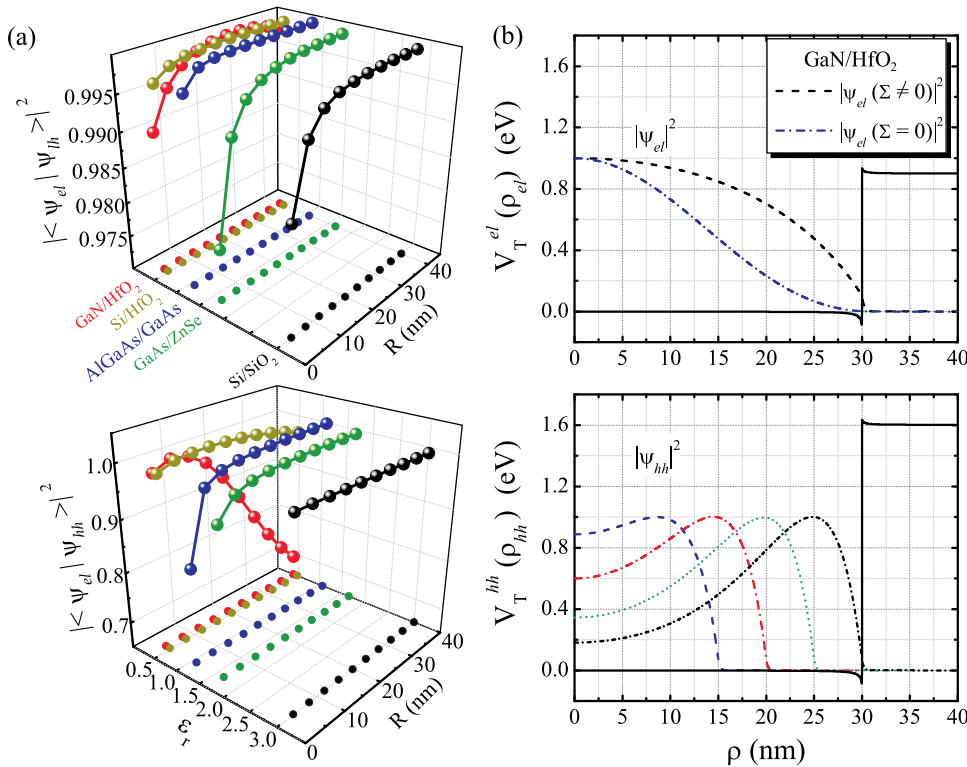


FIG. 2. (a) Overlap between the electron (el) and the light (lh) and heavy (hh) hole wave functions as a function of the core radius R , for several heterostructure materials with different ratios between dielectric constants ϵ_r , represented by different colors. (b) Effective confinement potentials V_T^i (solid) for $R = 30$ nm in the GaN/HfO₂ case for electrons and heavy holes, along with some examples of their wave functions. Electron wave functions are shown with (dashed) and without (dashed-dotted) taking image charge effects into account, for comparison. Hole wave functions (for $\Sigma \neq 0$) are depicted for $R = 15$ nm (blue dashed), 20 nm (red dash dotted), 25 nm (green dotted), and 30 nm (black short dash dotted).

confined at the interface, due to the cusp formed in this region by the self-energy potential (see black solid line). Note that as the radius increases, the hh wave function is squeezed towards the interface, explaining the increase of the energy in the heavy hole E_0 curve in Fig. 1(b). Due to its larger effective mass, as compared to that of the other charge carriers, the heavy hole is indeed expected to be more strongly confined in the interfacial cusps. Moreover, heavy holes in GaN/HfO₂ also have larger effective mass as compared to any charge carrier in Si/HfO₂, explaining why the interfacial confinement effect is weaker in the latter case.

Another interesting effect arising from the interfacial confinement in quantum wires comes from their topology: systems where the charge carriers are confined around a core are known to produce an interesting effect when a magnetic field is applied perpendicular to the confinement plane, namely, angular momentum transitions occur, even for the ground state, as the magnetic field intensity increases, which is reminiscent of the Aharonov-Bohm (AB) effect.⁹ In order to illustrate this, the electron and hole energy behaviors under such a magnetic field were numerically⁹ calculated and shown in Fig. 3 as a function of the field amplitude B for the GaN/HfO₂ NW. All the carriers have $E_0 < 0$, suggesting that their ground states are all interfacially confined. A large ($R = 30$ nm) radius is considered, in order to enhance the interfacial confinement effect (see Fig. 2(b)) and reduce the AB period, since this period is inversely proportional to the average radius of the carrier wave function. Indeed, the ground state energy exhibits AB oscillations for all carriers in this case, although they are much more evident for the hh . Due to their considerably smaller effective masses,¹⁵ el and lh are just weakly confined in the interface and still have a large wave function tail spreading inside the core, explaining the large AB period. The first ground state transition for these carriers is not so visible in Figs. 3(a) and 3(b) and

occurs at $B \approx 6$ T. On the other hand, for the hh , the AB transitions are quite clear, occurring at smaller magnetic fields, with a period $B \approx 2.5$ T. One easily verifies that the results neglecting the self-energy term in Fig. 3(d) are qualitatively different, showing a more conventional behavior with the magnetic field for a core-shell NW, namely, without angular momentum transitions for the ground state.

The interfacial confinement is also expected to have an important role on the electrons mobility along the core axis since this property depends on the electrons density in the central region of the wire, which is suppressed in the case of interfacial confinement. However, a more detailed investigation on this issue is left for future works.

In summary, we have theoretically investigated the charge carrier confinement in core-shell nanowires with

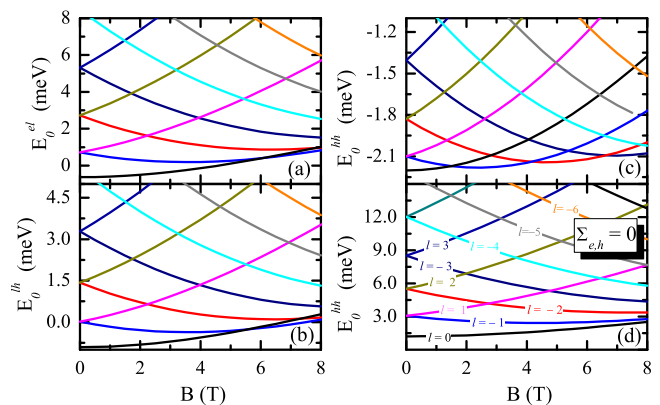


FIG. 3. Confinement energies as a function of the magnetic field for (a) electrons, (b) light, and (c) heavy holes, considering $n = 1$ and different values of angular momentum index l , in a $R = 30$ nm GaN/HfO₂ NW. (d) The results for a heavy hole in the same system, but neglecting image charge effects.

strong dielectric mismatch. Our results predict that, for specific configurations of the system, the carriers may be confined at the core-shell interface. Such interfacial confinement leads to drastic modifications on the electronic properties of the NW, especially under an applied magnetic field, where angular momentum transitions occur for the ground state, due to the AB effect. A decrease in the oscillator strength of the electron-hole pairs in $\epsilon_r < 1$ core-shell quantum wires is also predicted for larger wire radii, which directly affects their recombination rates. We believe that our results will spur on future experimental investigations on core-shell wires made out of high-k materials, contributing for a better understanding of these systems.

This work has received financial support from the Brazilian National Research Council (CNPq), CAPES, PRONEX/CNPq/FUNCAP, and FAPEMAT (Process No. 39788/2009).

¹P. Mohan, J. Motohisa, and T. Fukui, *Nanotechnology* **16**, 2903 (2005).

²A. I. Persson, M. W. Larsson, S. Stenstrom, B. J. Ohlsson, L. Samuelson, and L. R. Wallenberg, *Nano Mater.* **3**, 677 (2004).

- ³C. Chen, S. Shehata, C. Fradin, R. LaPierre, C. Couteau, and G. Weihs, *Nano Lett.* **7**, 2584 (2007).
- ⁴D. Tsvion, M. Schwartzman, R. P. Biro, P. Huth, and E. Joselevich, *Science* **333**, 1003 (2011).
- ⁵D. Jena and A. Konar, *Phys. Rev. Lett.* **98**, 136805 (2007).
- ⁶X. Zhu, Q. Li, D. E. Ioannou, D. Gu, J. E. Bonevich, H. Baumgart, J. S. Suehle, and C. A. Richter, *Nanotechnology* **22**, 254020 (2011).
- ⁷X. Jiang, Q. Xiong, S. Nam, F. Qian, Y. Li, and C. M. Lieber, *Nano Lett.* **7**, 3214 (2007).
- ⁸B. Li, B. Partoens, F. M. Peeters, and W. Magnus, *Phys. Rev. B* **79**, 085306 (2009).
- ⁹J. C. e Silva, A. Chaves, J. A. K. Freire, V. N. Freire, and G. A. Farias, *Phys. Rev. B* **74**, 085317 (2006).
- ¹⁰A. F. Slachmuylders, B. Partoens, W. Manus, and F. M. Peeters, *Phys. Rev. B* **74**, 235321 (2006).
- ¹¹See supplementary material at <http://dx.doi.org/10.1063/1.4720402> for more details about our calculations.
- ¹²T. A. S. Pereira, J. S. de Sousa, J. A. K. Freire, and G. A. Farias, *J. Appl. Phys.* **108**, 054311 (2010).
- ¹³J.-H. Kang, Q. Gao, H. J. Joyce, H. H. Tan, C. Jagadish, Y. Kim, Y. Guo, H. Xu, J. Zou, M. A. Fickenscher, L. M. Smith, H. E. Jackson, and J. M. Yarrison-Rice, *Cryst. Growth Des.* **11**, 3109 (2011).
- ¹⁴T. A. S. Pereira, J. S. de Sousa, G. A. Farias, J. A. K. Freire, M. H. Degani, and V. N. Freire, *Appl. Phys. Lett.* **87**, 171904 (2005).
- ¹⁵T. A. S. Pereira, J. A. K. Freire, V. N. Freire, G. A. Farias, L. M. R. Scolfaro, J. R. Leite, and E. F. da Silva, *Appl. Phys. Lett.* **88**, 242114 (2006).